Journal of Nuclear Science and Technology

ISSN: 0022-3131 (Print) 1881-1248 (Online) Journal homepage: http://www.tandfonline.com/loi/tnst20

Radon and thoron progeny integrated measurement based on high-voltage sampling

Lu Guo, Volkmar Schmidt, Oliver Meisenberg, Qiuju Guo & Jochen Tschiersch

To cite this article: Lu Guo, Volkmar Schmidt, Oliver Meisenberg, Qiuju Guo & Jochen Tschiersch (2016) Radon and thoron progeny integrated measurement based on high-voltage sampling, Journal of Nuclear Science and Technology, 53:12, 1999-2005, DOI: 10.1080/00223131.2016.1179137

To link to this article: http://dx.doi.org/10.1080/00223131.2016.1179137

JOURNAL OF NUCLEAR SCIENCE AND TECHNOLOGY, 2016
VOL. 53, NO. 12, 1999–2005
http://dx.doi.org/10.1080/00223131.2016.1179137

Radon and thoron progeny integrated measurement based on high-voltage sampling

Lu Guo[a,b], Volkmar Schmidt[c], Oliver Meisenberg[b,†], Qiuju Guo[a] and Jochen Tschiersch[b]

[a]State Key Laboratory of Nuclear Physics and Technology, School of Physics, Peking University, Beijing, China; [b]Institute of Radiation Protection, Helmholtz Zentrum München, German Research Center for Environmental Health (HMGU), Neuherberg, Germany; [c]Radon Calibration Laboratory, Federal Office for Radiation Protection, Bundesamt für Strahlenschutz (BfS), Berlin, Germany

ABSTRACT

For the purpose of directly measuring radon and thoron progeny concentrations simultaneously, an unattended battery-operated progeny measurement (UBPM) device, which samples aerosol particles in an electric field, was improved by adopting two different thickness aluminum foils for alpha particles discriminating. The equations for the calculation of the results were derived, and a series of calibration experiments and comparison tests were carried out in the potential alpha energy concentration calibration chamber in BfS Berlin and the HMGU experimental thoron house, respectively. Results show that the calibration coefficients are stable in different levels of radon and thoron progeny. The lower level detection limits of the device for radon and thoron progeny concentration are 1.22 and 0.14 Bq m^{-3}, respectively, for three months exposure. The instrument proved to be independent from environmental conditions in ordinary living room conditions (humidity <65% RH, aerosol particle concentration >1500 cm^{-1}). Comparison results show that the measurement results of the UBPM device are comparable with the reference instrument and suitable for long-term radon and thoron survey in dwellings.

ARTICLE HISTORY
Received 21 December 2015
Accepted 12 April 2016

KEYWORDS
Radon; thoron progeny; integrated measurement; high-voltage sampling; CR-39

1. Introduction

Radon (^{222}Rn) is an inert radioactive gas coming from the decay of ^{226}Ra which exist almost everywhere. Radon decays into a series of short-lived decay products, which can be inhaled into the human lung and cause internal exposure. Radon and radon progeny contribute almost half of the exposure dose to human beings from natural sources [1].

Thoron (^{220}Rn), an isotope of radon, is a decay product of thorium series and an inert radioactive gas also. Due to its short half-life (55.6 s) and the lack of field survey methods, its exposure dose was usually ignored. However, recently several field investigation data showed that in some areas radiation exposure contributed by thoron and its progeny is comparable to that of radon and its progeny [2–8].

Because exposure dose mainly comes from radon and thoron progenies instead of radon or thoron gas, the direct measurement of radon and thoron progeny is more preferred for the purpose of dose evaluation [8,9].

Traditional radon and thoron progeny measurement methods could be divided into two kinds, "active method" and "passive method". Active methods generally sample radon and thoron progeny by pumps, and use electronic detectors for radioactive particle measuring. It is commonly used in commercial devices, like BWLM-PLUS-2S (TracerLab, Germany), and WLx (Pylon, Canada) for continuous measurement. But active devices are noisy and power supply dependent. The passive sampling and measurement method, without the usage of electrical power, having the advantage of long measurement times, used to be favored by researchers. Zhuo et al. developed the low-cost, time-integrating thoron progeny measurement method based on the track-etching technique and passive deposition [10]. Mishra et al. developed the direct thoron progeny sensor for estimating equilibrium equivalent thoron concentration (EEC_{Tn}) which also could be used for radon progeny measurement, and studied its response to various aerosol concentrations and ventilation rates [11–14]. Li et al. analyzed the influence of environmental factors on thoron progeny deposition velocity and carried out a series of validation measurements using a new developed device [15]. Among those measurement devices, solid-state nuclear track detectors, such as CR-39 or LR115, are usually adopted as detectors, and the integrating measurement time is usually as long as three months, which is suitable for field survey of indoor environment.

However, the deposition velocity varies a lot in different environment, which limited the use of those devices. To improve this problem, Gierl et al. and Bi et al. developed an unattended battery-operated progeny measurement (UBPM) device for integrating thoron progeny measurement, which collected charged thoron

CONTACT Lu Guo guolu@pku.edu.cn
[†]Present address: Bundesamt für Strahlenschutz (BfS), Ingolstädter Landstr. 1, 85764 Neuherberg, Germany.

progeny by electric field and alpha particles emitted from ^{212}Po was registered by CR-39s [16,17]. The precipitation velocity of thoron progeny was proved to be independent from the relevant environmental parameters under a high-voltage electric field [17].

The aim of this work is to improve the UBPM device to measure radon and thoron progeny directly and simultaneously as well. Details of changes on the device and its theoretical algorithm derivation were studied. Besides, calibration of this device in a radon chamber and a thoron experimental house, comparison test and environmental sensitivity tests were also performed.

2. Materials and methods

2.1. The UBPM device

The photograph and sketch map of the improved unattended battery-operated thoron progeny measurement device (UBPM) are shown in Figure 1.

The UBPM device has two parts, the high-voltage generator part and the hemisphere detector part. First, in the bottom of the device, the 3.6 V from a lithium ion battery is transferred to 7 kV high voltages by a high-voltage converter. Second, in the upper part, a hemisphere wire-mesh of stainless steel with a diameter of 9 cm covers the detector assembly. Four square CR-39s (Radosys, Ltd, Hungary) with the size of 1 cm × 1 cm lie in the middle of hemisphere, while two different Al foils are tightened immediately over the CR-39 detectors with a circular plastic ring, just as shown in Figure 1 . The 7 kV high voltage is connected to the Al foils, whereas the wire-mesh is on ground potential. The high-voltage electric field inside the hemisphere chamber makes the negatively charged and neutral radon and thoron decay products collected on the surface of the Al foils. The alpha particles emitted from the radon and thoron progeny are recorded by the CR-39s if they penetrate the Al foils.

In order to measure radon and thoron progeny concentrations simultaneously, two kinds of aluminum foils with thicknesses of 25 and 35 μm (AL000392 and AL000370, Goodfellow GmbH, Germany; purity: 99.0%) are used to discriminate those alpha particles emitted from radon and thoron decay products. Two CR-39s covered by 25 μm Al foil are named "the 1st Part", while the other two CR-39s covered by 35 μm Al foil are named "the 2nd Part".

Table 1 shows properties of all the relevant alpha particle-emitting isotopes in both radon and thoron series. The ranges of different alpha particle in pure Al materials were calculated using the Monte Carlo particle track software TRIM [18]. Because of its short half-life, ^{216}Po (from the thoron series, emitting alpha particles of 6.8 MeV) is sampled only to negligible activity on the Al foils. The range of 6.00 MeV alpha particle from ^{218}Po and 6.05 MeV alpha particles from ^{212}Bi in aluminum are 27.9 and 28.2 μm, respectively. Considering more energy lose due to large incident angle and the minimum detectable energy of CR-39s, 0.75 MeV [19], it can be assumed that the 6.00 and 6.05 MeV alpha particles cannot be recorded by the CR-39s. The range of 7.69 MeV alpha particle from ^{214}Po and 8.78 MeV alpha particles from ^{212}Po in aluminum is 40.5 and 49.6 μm, so they could be recorded by the four CR-39s, with a lower sensitivity in the second part.

2.2. The calculation of radon and thoron progeny concentration

The parts of radon and thoron progeny which are sampled in the electric field accumulate to steady-state activities on the substrates according to their half-lives. Thus, after enough time of decay, they finally contribute to the activity of ^{214}Po and ^{212}Po and their alpha particle emissions, respectively, which can be measured in the CR-39 detectors. According to the study of Bi et al. [17], it could be assumed that the collection efficiency η_c is the same for all the progenies and will not be affected by environmental factors.

In the first part, alpha particle from ^{214}Po (7.69MeV) and ^{212}Po (8.78MeV) could be recorded by CR-39s. We assume that the detection efficiency of 7.69 MeV alpha in the first part is $\eta_{dPo-214}$, while the detection efficiency of 8.78 MeV alpha is $\eta_{dPo-212}$, respectively. The relationship of the track densities of CR-39s in the first part and the concentrations of radon and thoron decay products could be expressed as follows:

$$D_1 = \eta_c \cdot v_{\text{eff}} \cdot \frac{T}{S} \cdot \left[\eta_{dPo-214} \cdot \left(r \cdot \frac{C_{Po-218}}{\lambda_{Po-218}} + \frac{C_{Pb-214}}{\lambda_{Pb-214}} + \frac{C_{Bi-214}}{\lambda_{Bi-214}} \right) + \eta_{dPo-212} \cdot \left(\frac{C_{Pb-212}}{\lambda_{Pb-212}} + \frac{C_{Bi-212}}{\lambda_{Bi-212}} \right) \right]. \quad (1)$$

A list of explanation of all the parameters is shown in Table 2.

r refers to the percentage of originating ^{214}Pb which remain on the Al foil, as part of the ^{214}Pb decay from ^{218}Po will leave the Al foil due to recoil and possible positive charge.

As for "the 2nd part", the relationship between the track densities and radon and thoron decay products concentrations could be expressed as follows:

$$D_2 = \eta_c \cdot v_{\text{eff}} \cdot \frac{T}{S} \cdot \left[\eta'_{dPo-214} \cdot \left(r \cdot \frac{C_{Po-218}}{\lambda_{Po-218}} + \frac{C_{Pb-214}}{\lambda_{Pb-214}} + \frac{C_{Bi-214}}{\lambda_{Bi-214}} \right) + \eta'_{dPo-212} \cdot \left(\frac{C_{Pb-212}}{\lambda_{Pb-212}} + \frac{C_{Bi-212}}{\lambda_{Bi-212}} \right) \right]. \quad (2)$$

Because of the thicker thickness of Al foils, the detection efficiencies are smaller than those in the first part.

On the other side, the equilibrium equivalent concentrations of radon and thoron decay products could be expressed as [1]

$$\begin{aligned} \text{EEC}_{\text{Rn}} &= 0.105 \cdot C_{Po-218} + 0.515 \cdot C_{Pb-214} + 0.380 \cdot \\ C_{Bi-214} &= 0.105 \cdot C_{Po-218} \\ &\quad + 3.203 \times 10^{-4} \cdot \left(\frac{C_{Pb-214}}{\lambda_{Pb-214}} + \frac{C_{Bi-214}}{\lambda_{Bi-214}} \right), \quad (3) \end{aligned}$$

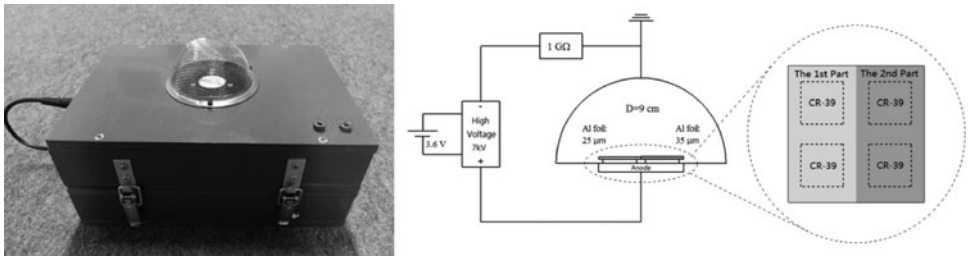

Figure 1. Photograph and sketch map of the improved UBPM device.

$$\mathrm{EEC_{Tn}} = 0.913 \cdot C_{Pb-212} + 0.087 \cdot C_{Bi-212} = 1.669 \times 10^{-5} \cdot \left(\frac{C_{Pb-212}}{\lambda_{Pb-212}} + \frac{C_{Bi-212}}{\lambda_{Bi-212}} \right). \quad (4)$$

From Equation (4), we can easily find that $\frac{C_{Pb-212}}{\lambda_{Pb-212}} + \frac{C_{Bi-212}}{\lambda_{Bi-212}}$ is proportional to $\mathrm{EEC_{Tn}}$. Taking the proportional coefficient as B ($= 6.0 \times 10^4$s), $\frac{C_{Pb-212}}{\lambda_{Pb-212}} + \frac{C_{Bi-212}}{\lambda_{Bi-212}} = B \cdot \mathrm{EEC_{Tn}}$ can be derived.

In the following, it is assumed that the ratio of the activity concentrations of the three radon progenies is constant. Then, $c_{Po\text{-}218}$ is proportional to the activity concentration of the other two radon progenies. Consequently, from Equation (3), we can find that $r \cdot \frac{C_{Po-218}}{\lambda_{Po-218}} + \frac{C_{Pb-214}}{\lambda_{Pb-214}} + \frac{C_{Bi-214}}{\lambda_{Bi-214}}$ is proportional to $\mathrm{EEC_{Rn}}$. Making A to be the proportional coefficient, that makes $r \cdot \frac{C_{Po-218}}{\lambda_{Po-218}} + \frac{C_{Pb-214}}{\lambda_{Pb-214}} + \frac{C_{Bi-214}}{\lambda_{Bi-214}} = A \cdot \mathrm{EEC_{Rn}}$.

Taking those linear relationships into Equations (1) and (2), it could be rewritten as follows:

$$\mathrm{D_1} = \eta_c \cdot \upsilon_{\mathrm{eff}} \cdot \frac{T}{S} \cdot \left[\eta_{dPo-214} \cdot A \cdot \mathrm{EEC_{Rn}} + \eta_{dPo-212} \cdot B \cdot \mathrm{EEC_{Tn}} \right] = \left(e_{1R} \cdot \mathrm{EEC_{Rn}} + e_{1T} \cdot \mathrm{EEC_{Tn}} \right) \cdot T, \quad (5)$$

$$\mathrm{D_2} = \eta_c \cdot \upsilon_{\mathrm{eff}} \cdot \frac{T}{S} \cdot \left[\eta'_{dPo-214} \cdot A \cdot \mathrm{EEC_{Rn}} + \eta'_{dPo-212} \cdot A \cdot \mathrm{EEC_{Rn}} \right] = \left(e_{2R} \cdot \mathrm{EEC_{Rn}} + e_{2T} \cdot \mathrm{EEC_{Tn}} \right) \cdot T, \quad (6)$$

where $e_{1R} = \eta_c \cdot \upsilon_{\mathrm{eff}} \cdot \eta_{dPo-214} \cdot A/S$, $e_{1T} = \eta_c \cdot \upsilon_{\mathrm{eff}} \cdot \eta_{dPo-212} \cdot B/S$, $e_{2R} = \eta_c \cdot \upsilon_{\mathrm{eff}} \cdot \eta'_{dPo-214} \cdot A/S$, $e_{2T} = \eta_c \cdot \upsilon_{\mathrm{eff}} \cdot \eta'_{dPo-212} \cdot B/S$. Those four coefficients are constant with unit of tracks $\mathrm{mm^{-2}}$/(Bq $\mathrm{m^{-3}}$ s).

Being rewritten in matrix form, the relation between the track densities recorded by CR-39s of the two parts and the $\mathrm{EEC_{Rn}}$ and $\mathrm{EEC_{Tn}}$ can be expressed as equation below

$$\begin{bmatrix} D_1 \\ D_2 \end{bmatrix} = T \cdot \begin{bmatrix} e_{1R} & e_{1T} \\ e_{2R} & e_{2T} \end{bmatrix} \begin{bmatrix} \mathrm{EEC_{Rn}} \\ \mathrm{EEC_{Tn}} \end{bmatrix}. \quad (7)$$

The matrix coefficients e_{1R}, e_{2R}, e_{1T}, e_{1T} could be derived through calibration.

2.3. Determination of the coefficients

In order to determine the four coefficients, calibration measurements were performed in the potential alpha energy concentration calibration chamber (PAEC chamber) in the federal office for radiation protection

Table 1. Properties of alpha-emitting isotopes in radon and thoron series.

Decay chain	Isotope	Alpha energy MeV	Half-life	Range in Al μm
Radon	Rn-222	5.49	3.82 d	24.5
	Po-218	6.00	3.10 m	27.9
	Po-214	7.96	164.3 μs	40.5
Thoron	Rn-220	6.29	55.6 s	29.9
	Po-216	6.78	0.145 s	33.5
	Bi-212	6.05	60.6 m	28.2
	Po-212	8.78	0.299 μs	49.6

Table 2. Symbol and unit of parameters in the equations.

Parameter	Description	Unit
$\mathrm{D_1}$, $\mathrm{D_2}$	Net track density of the first part and the second part	Tracks $\mathrm{mm^{-2}}$
η_c	Collection efficiency	
υ_{efl}	Effective sampling flow rate	$\mathrm{m^3/s}$
T	Exposure time	s
S	Area of CR-39s	$\mathrm{mm^2}$
η_{di}*	Detection efficiency of *i* in the first part	
η'_{di}	Detection efficiency of *i* in the second part	
r	Percentage of remain ^{214}Pb on the Al foil	
C_i	Activity concentrations of *i*	Bq $\mathrm{m^{-3}}$
λ_i	Decay constants of *i*	$\mathrm{s^{-1}}$

*i = Po-218, Pb-214, Bi-214, Pb-212, Bi-212.

Table 3. Radon progeny calibration results in the PAEC chamber.

	D_1/T tracks mm^{-2} d^{-1}	D_2/T tracks mm^{-2} d^{-1}	EEC_{Rn}* Bq m^{-3}	e_{1R} tracks mm^{-2} (Bq m^{-3} d)$^{-1}$	e_{2R} tracks mm^{-2} (Bq m^{-3} d)$^{-1}$
1	130.8	18.5	4464 ± 94	0.0283	0.00400
2	155.4	24.2	5113 ± 52	0.0294	0.00458
3	613.1	95.2	19,666 ± 607	0.0301	0.00468
Mean ± SD				0.0293 ± 0.0007	0.00442 ± 0.0003

*EEC_{Rn} was measured by the quality assured reference method.

(BfS) in Berlin [20] and thoron experimental house in HMGU [21].

The PAEC chamber was used for the calibration for short-lived ^{222}Rn progeny with a volume of 30 m^3. Stable radon progeny and aerosol concentration could be realized in the chamber by controlling the radon gas and aerosol source automatically. The radon decay products concentration could be measured using the quality assured reference measurement of the calibration laboratory accredited by the German accreditation service (DAkkS). The reference value is traced back to the German national normal at the Physikalisch Technische Bundesanstalt (PTB), Braunschweig.

The HMGU thoron experimental house was constructed in a laboratory room of Helmholtz Zentrum München. The single room house (7.1 m^3) was built from unfired clay stones and clay plaster, with ^{232}Th enriched granite powder mixed clay for the inner side, so it could provide conditions with relative high concentration of not only radon but also thoron. A working level monitor BWLM-PLUS-2S (TracerLab, Germany) was used as a secondary reference instrument traceable to the German national standard.

Radon progeny coefficients (e_{1R},e_{2R}) calibration experiments were performed in the PAEC chamber. During calibration experiments, the aerosol concentration was changing between 1800 and 4680 cm^{-3}, the humidity was 33.6∼39.0% RH. The EEC_{Rn} was controlled from 4.5 to 19.7 kBq m^{-3}. The exposure time is 7 hours for each experiment.

Thoron progeny coefficients (e_{1T},e_{2T}) calibration experiments were performed in the HMGU thoron experimental house. During calibration experiments, the relative humidity was between 50% and 60% and the aerosol concentration was around 3000 cm^{-3}. The radon progeny concentration changed between 17 and 24 Bq m^{-3}, while the concentration of thoron progeny was 4∼7 Bq m^{-3}. The exposure time is from 70 to 120 hours each.

3. Results and discussions

3.1. Radon progeny calibration coefficients

Three calibration experiments were performed in the pure radon environment in the PAEC chamber with different radon progeny concentrations. The calibration results are shown in Table 3. D_1 and D_2 are the net tracks densities on CR-39s of the first part and the second part separately, which were read under RadoMeter Microscope (Radosys, Ltd, Hungary) after been etched in NaOH solution (860 g NaOH, 3400 g water, 94 °C, 4 hour). The EEC_{Rn} is the reference radon progeny concentration which is given by the PAEC chamber.

The radon progeny calibration coefficients in the first part and the second part are shown in the fifth and sixth column. From the experiment results, we find that the radon progeny coefficients (e_{1R},e_{2R}) are rather stable. Because the thickness of the Al foil in the second part is 35 μm which is thicker than that in the first part (25 μm), the e_{2R} is quite smaller than e_{1R}.

The average value of e_{1R} and e_{2R} is 0.0293 and 0.00442 tracks mm^{-2} /(Bq m^{-3} d) with the uncertainty shown in Table 3.

3.2. Thoron progeny calibration coefficients

Three calibration experiments were performed in the thoron experimental house in HMGU. Using the radon progeny coefficients in Table 3 and the EEC_{Rn} measured by BWLM-PLUS-2S, the radon progeny's contribution to D_1 and D_2 could be easily deduced. Then, the thoron progeny coefficients could be calculated using the net

Table 4. Thoron progeny calibration results in the HMGU house.

	D_2/T tracks mm^{-2} d^{-1}	D_2/T tracks mm^{-2} d^{-1}	EEC_{Rn}* Bq m^{-3}	EEC_{Tn} Bq m^{-3}	e_{1T} tracks mm^{-2} (Bq m^{-3} d)$^{-1}$	e_{2T} tracks mm^{-2} (Bq m^{-3} d)$^{-1}$
1	1.58	0.73	23.41 ± 1.08	4.53 ± 0.10	0.195	0.138
2	2.24	0.87	19.44 ± 1.17	6.95 ± 0.12	0.239	0.112
3	2.09	0.93	24.09 ± 1.13	5.92 ± 0.11	0.233	0.138
Mean ± SD					0.222 ± 0.020	0.129 ± 0.012

*EEC_{Rn} and EEC_{Tn} was measured by BWLM-PLUS-2S.

Table 5. Comparison test results in the thoron experimental house.

Test no.	BWLM-PLUS-2S (reference instrument)		UBPM		Deviation	
	EEC_{Rn} Bq m^{-3}	EEC_{Tn} Bq m^{-3}	EEC_{Rn}* Bq m^{-3}	EEC_{Tn} Bq m^{-3}	EEC_{Rn}	EEC_{Tn}
1	17.2 ± 1.02	4.9 ± 0.10	22.3 ± 5.6	4.7 ± 1.2	29.7%	4.7%
2	16.3 ± 1.47	6.6 ± 0.51	23.7 ± 6.0	4.3 ± 1.0	45.1%	35.4%
3	10.6 ± 1.00	2.9 ± 0.25	12.4 ± 3.1	2.7 ± 0.7	17.0%	6.9%

*25% relative uncertainty is mainly contributed by CR-39 [22,23].

track densities and EEC_{Tn}. The calibration results are shown in Table 4.

It could be found that the thoron progeny coefficients (e_{1T},e_{2T}) seem to be stable under different radon and thoron mixed progeny conditions. Because the thickness of the Al foil in the second part is 35 μm, which is thicker than that in the first part (25 μm) and the range of 8.78 MeV alpha particle is 49.6 μm, the e_{2T} is smaller than e_{1T}, but the difference is not so obvious as e_{1R} and e_{2R}.

The average value of e_{1T} and e_{2T} are 0.222 and 0.129 tracks mm^{-2}/(Bq m^{-3} d), respectively, with the uncertainty smaller than 10%.

3.3. The low level detection limits of radon and thoron progeny concentration

Taking the radon and thoron progeny calibration coefficients e_{1R}, e_{2R}, e_{1T}, e_{2T} into Equation (7), the EEC_{Rn}, EEC_{Tn} could be calculated as follows for field indoor environment survey:

$$\begin{bmatrix} EEC_{Rn} \\ EEC_{Tn} \end{bmatrix} = \frac{1}{T} \cdot \begin{bmatrix} 0.0293 & 0.222 \\ 0.00442 & 0.129 \end{bmatrix}^{-1} \begin{bmatrix} D_1 \\ D_2 \end{bmatrix} = \frac{1}{T} \cdot \begin{bmatrix} 46.10 & -79.32 \\ -1.58 & 10.47 \end{bmatrix} \cdot \begin{bmatrix} D_1 \\ D_2 \end{bmatrix}. \quad (8)$$

Considering impurities of the aluminum foils with alpha particle-emitting radionuclides cause additional background tracks over the exposure time, the background density of CR-39 is 0.942 + 0.064 tracks/mm^2 [16]. At a confidence interval of 95%, the lower level detection limits of radon progeny and thoron progeny concentration are 1.22 and 0.14 Bqm^{-3}, respectively, for a measurement during three months.

3.4. Comparison experiments in the thoron experimental house

To test the new instrument, another three experiments were performed in the thoron experimental house, with the exposure time of nearly one week. The results of the comparison experiments are showed in Table 5.

The measurement results of the UBPM device are compared with the reference instrument BWLM-PLUS-2S which gives the average radon and thoron progeny concentrations over the test period. The results show that the EEC_{Rn} and EEC_{Tn} are comparable within a deviation of 30%, except measurement no. 2. The deviation of the radon progeny concentration is larger than that of thoron progeny concentration. The main reason is considered that the assumption of the constant radon progenies activity concentration ratio might not be accurate in all environments. The instability of CR-39 detectors could also be the reason. But the deviation is acceptable in long-term field measurement.

3.5. Sensitivity tests under different environmental conditions

During the calibration measurements in the PAEC chamber, the radon progeny coefficient (e_{1R},e_{2R}) proved to be stable in conditions with different radon progeny concentrations, humidity ranged from 33.6% to 39% RH and aerosol concentrations from 1800/cm^3 to 4600/cm^3. As aerosol particle concentrations, humidity, and turbulent states are important environmental factors which may strongly influence the efficiency of passive device, five more tests were also performed in the PAEC chamber to test the sensitivity of the UBPM device towards environmental factors. Environmental parameters during the tests are listed in Table 6.

Table 6. Environmental parameters in the PAEC chamber.

Test no.	EEC_{Rn} kBqm^{-3}	Humidity %	Aerosol cm^{-3}	Unattached fraction %	Turbulence
1	5.11 ± 0.05	35.0	1800 ± 70	2	Low
2	5.40 ± 0.13	39.0	4700 ± 600	2	High
3	5.97 ± 0.14	71.8	4200 ± 300	1	Low
4	3.85 ± 0.09	78.8	220 ± 30	16	Low
5	2.73 ± 0.06	34.2	180 ± 20	24	Low
6	16.00 ± 0.75	36.3	360 ± 20	14	Low

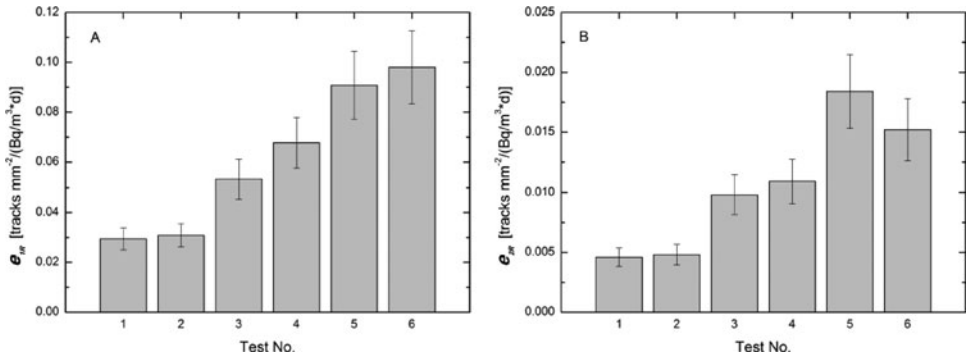

Figure 2. Coefficients of radon progeny in six environmental sensitivity tests. (A) Coefficients on "the 1st Part", e_{1R}, (B) coefficients on "the 2nd Part", e_{2R}.

Test 1 is one of the calibration measurements representing the normal living environment as reference condition, while the other five tests are changed conditions.

The coefficients of radon decay products on "the 1st Part" and "the 2nd Part" are showed respectively in Figure 2. Comparing the high humidity condition (test 3, 72% RH) with the reference condition (test 1, 35% RH), a slight increase of sensitivity was observed. Larger influence was caused by the very low aerosol concentrations connected with a very high fraction of unattached progeny (test 5, 6). Increased turbulence in test 2 had no influence on the performance of the instrument.

4. Conclusion

The UBPM device was improved to measure radon and thoron progeny concentrations simultaneously. The principle and algorithm derivation are given. Calibration experiments were performed in the PAEC chamber and the HMGU thoron experimental house and a series of comparison experiments were carried out.

Results show that both the radon and thoron progeny coefficients are stable in different levels of radon and thoron progeny concentration and the device is comparable with the reference instrument. The lower level detection limits of radon and thoron progeny concentration are 1.22 and 0.14 Bq m^{-3}, respectively, for three months exposure.

The sensitivity of the UBPM device in several extreme environmental conditions was tested. Results show that humidity higher than 70% RH and aerosol concentration lower than 400/cm^3 will influence the sampling efficiency of the instrument, while turbulent state of indoor air have no effect on it.

Because of its soundless operation, it is suggested the device is suitable for long-term indoor survey, in dwellings in which humidity will not exceed 65% RH and particle concentration is higher than 1500/cm^3, especially on the purpose of radon and thoron progeny dose evaluation.

For a further improvement, allowing faster and more accurate evaluation, alpha spectrometry is recommended to be used for alpha particle detection in this assembly.

Acknowledgments

The support of Lu Guo by the China Scholarship Council is gratefully acknowledged.

Disclosure statement

No potential conflict of interest was reported by the authors.

References

[1] UNSCEAR. Sources and effects of ionizing radiation. Sweden: UNSCEAR; 2000.
[2] Shang B, Chen B, Gao Y, et al. Thoron levels in traditional Chinese residential dwellings. Radiat Environ Biophys. 2005;44:193–199.
[3] Kim CK, Kim YJ, Lee HY, et al. ^{220}Rn and its progeny in dwellings of Korea. Radiat Meas. 2007;42:1409–1414.
[4] Kavasi N, Nemeth C, Kovacs T, et al. Radon and thoron parallel measurements in Hungary. Radiat Prot Dosim. 2007;123:250–253.
[5] McLaughlin J, Murray M, Currivan L, et al. Long-term measurements of thoron, its airborne progeny and radon in 205 dwellings in Ireland. Radiat Prot Dosim. 2011;145:189–193.
[6] Chen J, Bergman L, Falcomer R, et al. Results of simultaneous radon and thoron measurements in 33 metropolitan areas of Canada. Radiat Prot Dosim. 2014;163:1–7.
[7] Zhang L, Guo Q, Wang S. Dosimetric evaluation of thoron exposure in the three typical rural indoor environments of China. J Radioanal Nucl Chem. 2015;303:1565–1568.
[8] Gierl S, Meisenberg O, Feistenauer P, et al. Thoron and thoron progeny measurements in German clay houses. Radiat Prot Dosim. 2014;160:160–163.
[9] Janik M, Tokonami S, Kranrod C, et al. Comparative analysis of radon, thoron and thoron progeny concentration measurements. J Radiat Res. 2013;54:597–610.
[10] Zhuo W, Iida T. Estimations of thoron progeny concentrations in dwellings with their deposition rate measurements. Japan J Health Phys. 2000;35(3):365–370.

[11] Mishra R, Mayya YS. Study of a deposition based direct thoron progeny sensor (DTPS) technique for estimating equilibrium equivalent thoron concentration (EETC) in indoor environment. Radiat Meas. 2008;43:1408–1416.
[12] Mishra R, Prajith R, Sapra BK, et al. An integrated approach for the assessment of the thoron progeny exposures using direct thoron progeny sensors. Radiat Prot Dosim. 2010;141(4):363–366.
[13] Mishra R, Mayya YS, Kushwaha SH. Measurement of $^{220}Rn/^{222}Rn$ progeny deposition velocities on surfaces and their comparison with theoretical models. J Aerosol Sci. 2009;40:1–15.
[14] Mishra R, Prajith R, Sapra BK, et al. Response of direct thoron progeny sensors (DTPS) to various aerosol concentrations and ventilation rates. Nucl Instr Methods Phys Res B. 2010;268:671–675.
[15] Li H, Zhang L, Guo Q. The influence of environmental factors on the deposition velocity of thoron progeny. Radiat Prot Dosim. 2012;152:84–88.
[16] Gierl S, Meisenberg O, Haninger T, et al. An unattended device for high-voltage sampling and passive measurement of thoron decay products. Rev Sci Instr. 2014;85:022103.
[17] Bi L, Tschiersch J, Meisenberg O, et al. Development of a new thoron progeny detector based on SSNTD and the collection by an electric field. Radiat Prot Dosim. 2011;145:88–294.
[18] Ziegler JF, Biersack JP. TRIM – the transport of ions in matter. SRIM – the stopping and range of ions in matter software package, version 2013.00, 2013. Available from: http://www.srim.org
[19] Zhuo W Iida T. An instrument for measuring equilibrium-equivalent radon and thoron concentrations with etched track detectors. Health Phys. 1999;77:584–587.
[20] Hamel P, Schmidt V. The calibration laboratory for radon and radon decay products at the federal office for radiation protection in Germany. Kerntechnik. 2010;66:202–205.
[21] Tschiersch J, Meisenberg O. The HMGU thoron experimental house: a new tool for exposure assessment. Radiat Prot Dosim. 2010;141:395–399.
[22] Tschiersch J, Haninger T. Comments on "Adjusting Lung Cancer Risks for Temporal and Spatial Variations in Radon Concentrations in Dwellings in Gansu Province, China" by Lubin et al. (Radiat Res 163, 571–579, 2005). Radiat Res. 2006;166:120–121.
[23] Beck TR, Foerster F, Buchröder H, et al. The measurement accuracy of passive radon instruments. Radiat Prot Dosim. 2014;158:59–67.